Since January 2020 Elsevier has created a COVID-19 resource centre with free information in English and Mandarin on the novel coronavirus COVID-19. The COVID-19 resource centre is hosted on Elsevier Connect, the company's public news and information website.

Improved Cutaneous Genetic Immunization by Microneedle Array Delivery of an Adjuvanted Adenovirus Vaccine

Journal of Investigative Dermatology (2020) **140,** 2528–2531; doi:10.1016/j.jid.2020.03.966

TO THE EDITOR

Genetic immunization based on recombinant DNA technology is an attractive approach for induction of robust antiviral or antitumor immunity (Condon et al., 1996; He et al., 2006). Specifically, adenoviral vaccines encoding target antigen transgenes are the subject of extensive preclinical studies owing to their established capacity for generating immune responses (Kim et al., 2016; Zaric et al., 2019). The skin is an ideal vaccination site containing an innate immune network that is exquisitely responsive to environmental stimuli and capable of inducing a proinflammatory microenvironment favoring the generation of strong and long-lasting adaptive immunity (Kabashima et al., 2019; Kashem et al., 2017). To exploit the readily accessible cutaneous immune network, vaccine delivery technologies, such as microneedle arrays (MNAs), have been developed to precisely and reproducibly target immunologically active cargos to skin microenvironments (Kim et al., 2012; Sullivan et al., 2010).

Though often effective in inducing antibody responses, traditional vaccines frequently fail to generate robust cytotoxic T-cell responses that are essential to prevent or treat many cancers or infectious diseases. Currently, induction of antigen-specific cellular immunity is a point of emphasis in the vaccine field, as evidenced by recent efforts to generate universal vaccines for mutable infectious agents (e.g., influenza, HIV, and coronaviruses). These vaccines target infected cells expressing functionally essential viral antigens, instead of, or in addition to, more traditional viral surface proteins that are targeted by antibodies but are highly mutable (Herold and Sander, 2020). Successful integration of adenovector vaccines onto coated or into dissolvable MNAs has been shown to induce efficacious and durable antigen-specific responses in preclinical studies (Bachy et al., 2013; DeMuth et al., 2013; Vrdoljak et al., 2012). Despite these promising results, clinical translation of adenovector vaccines has been hampered by limited efficacy, thereby defining an unmet need to enhance the immune responses induced by adenovirus vaccines. Here, we generated a three-dimensional multicomponent skin-targeted vaccine platform, combining an adenovirus-encoded antigen with an adjuvant to induce stronger cellular immune responses. Specifically, we developed dissolving MNAs to simultaneously co-deliver adenovectors encoding the transgene for the model antigen ovalbumin (OVA) together with polyinosinic acid:polycytidylic acid (Poly[I:C]), a toll-like receptor (TLR) 3–triggering double-stranded RNA molecule, to the cutaneous microenvironment, with the primary goal of enhancing antigen-specific cellular immune responses. Dissolvable MNAs are designed to mechanically penetrate the superficial cutaneous layers, rapidly dissolve upon insertion into the skin, and deliver uniform quantities of biocargo to a defined three-dimensional space within the skin (Korkmaz et al., 2015). They enable localized delivery of low amounts of drugs or vaccines to achieve high concentrations in a specific skin microenvironment.

Innate cell-signaling pathways (e.g., downstream of TLRs) are well-studied targets for the rational design of vaccine adjuvants for protein subunit vaccines (Schijns and O'Hagan, 2006); however, they have yet to be comprehensively evaluated in the context of recombinant viral vectored vaccines because of significant mechanistic differences, including differences in the kinetics and amount of antigen expression. Among TLR family members, TLR3 signaling imparts unique responses, such as secretion of immunostimulatory IFN-β and CXCL10, owing to its distinct downstream pathways. Although other TLRs signal through adaptor protein MyD88, TLR3 uses the TRIF adapter protein, with subsequent activation of IFN regulatory transcription factor 3 and IFN regulatory transcription factor 7 (Boehme and Compton, 2004; Schijns and O'Hagan, 2006). Here, using in vivo mouse models, we demonstrate that MNA delivery of the TLR3 agonist Poly(I:C) with antigen-encoding adenovectors results in proinflammatory changes in the targeted skin microenvironment that correlate with robust antigen-specific cellular and humoral adaptive immune responses. For these studies, mice were used at 8–10 weeks of age, and all experiments were conducted in accordance with Institutional Animal Care and Use Committee-approved protocols and guidelines.

Dissolvable MNAs incorporating adenovirus vaccines (Ad5.OVA) with or without Poly(I:C) were manufactured using a composition of two generally-regarded-as-safe water-soluble biomaterials, carboxymethyl cellulose and trehalose. Optical microscopy images of MNAs before and after in vivo application to skin demonstrated high-quality micron-scale needles after fabrication and effective dissolution upon skin insertion, respectively (Figure 1a and b). Importantly, the multicomponent MNAs effectively delivered adenovirus (Figure 1c) and Poly(I:C) (Figure 1d) to the skin microenvironment in vivo (Figure 1e), resulting in transgene (OVA) expression (Figure 1f). Interestingly, compared with MNA delivery of adenovector alone, inclusion of Poly(I:C)

Abbreviations: MNA, microneedle array; OVA, ovalbumin; Poly(I:C), polyinosinic acid:polycytidylic acid; TLR, toll-like receptor

Accepted manuscript published online 21 April 2020; corrected proof published online 24 June 2020

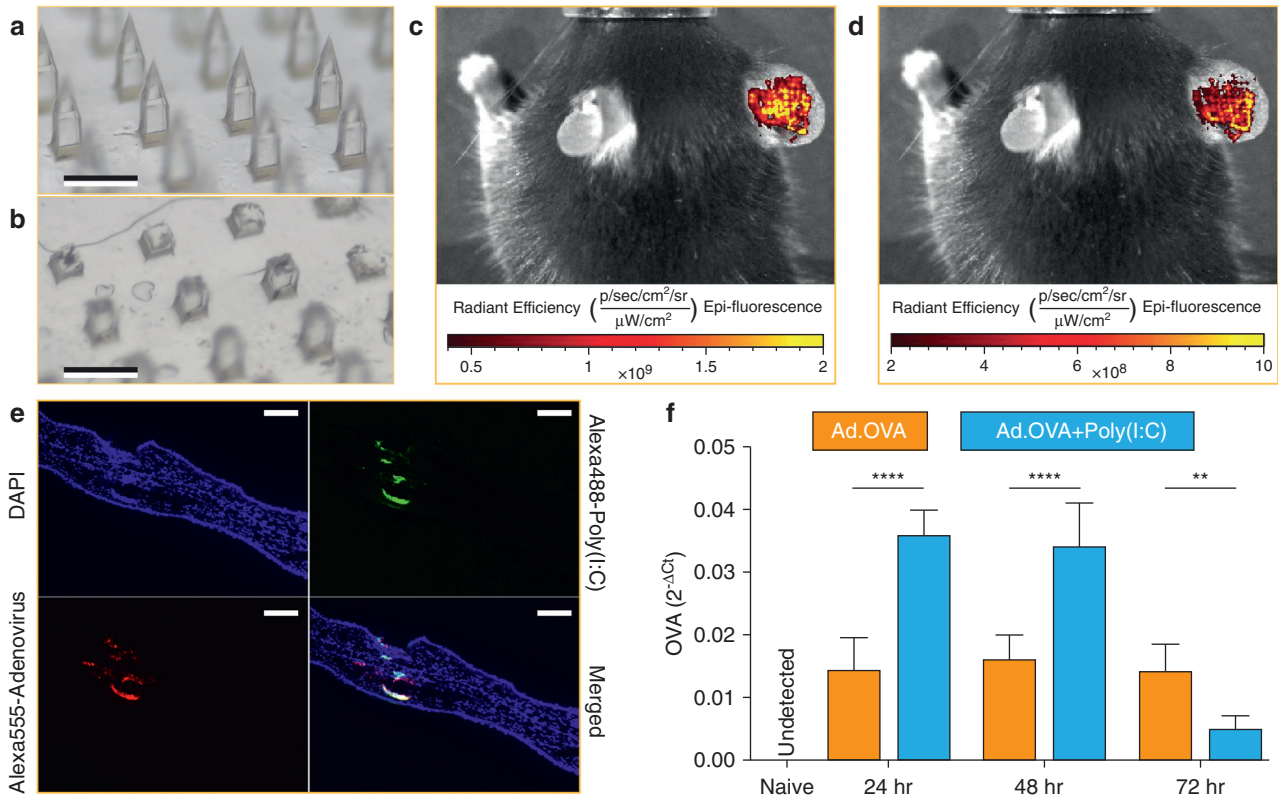

Figure 1. MNAs effectively penetrate the skin and deliver live adenovector vaccines and Poly(I:C) to the same cutaneous microenvironment, driving robust antigen transgene expression. Dissolvable MNAs incorporating Ad.OVA ± Poly(I:C) were fabricated using a spin-casting method, applied to the mouse skin for 10 minutes, and then removed. Images of MNAs **(a)** before and **(b)** after the application were obtained using optical stereomicroscopy. Bar = 500 µm. In vivo multicomponent vaccine delivery performance of MNAs was evaluated by fluorescent live animal imaging following application of MNAs incorporating Alexa488-labeled Poly(I:C) and Alexa555-labeled Ad.OVA to the right ears of mice. Mice were imaged using the IVIS 200 system with filters corresponding to **(c)** Alexa488 and **(d)** Alexa555 to demonstrate simultaneous co-delivery of Ad.OVA and Poly(I:C). **(e)** MNA-treated mouse skin was excised and imaged by epifluorescent microscopy and bright-field microscopy to show the intercutaneous delivery of multicomponent vaccines in vivo. Bar = 100 µm. **(f)** To quantify transgene (OVA) expression in the skin, mouse skin that was treated with Ad.OVA ± Poly(I:C) MNAs was recovered after 24, 48, and 72 hours, and OVA mRNA expression in the skin was quantified by RT-qPCR. Data are presented as mean ± SD. Significance was determined by two-way ANOVA followed by Sidak multiple comparison test. $^{**}P < 0.01$ and $^{****}P < 0.0001$. MNA, microneedle array; OVA, ovalbumin.

was associated with significantly increased expression of OVA mRNA that was sustained through 48 hours ($P < 0.0001$).

Intercutaneous vaccination with MNAs generated robust antigen-specific cytotoxic and humoral-immune responses. Remarkably, multicomponent MNA vaccine platforms incorporating both antigen-encoding adenovector and Poly(I:C) augmented OVA-specific lytic immunity by approximately two-fold compared with MNA delivery of the same adenovector alone (Figure 2a). In addition to cell-mediated immunity, MNA-adenovirus vaccine platforms with or without the addition of Poly(I:C) elicited strong and robust antigen-specific antibody responses (IgG1 and IgG2c) (Figure 2b and c). Thus, adding Poly(I:C) to this MNA-delivered adenovirus vaccine significantly improved antigen-specific cellular immunity while maintaining strong antibody responses. Notably, multicomponent MNAs integrating both Poly(I:C) and adenovirus retained their immunogenicity after 1 month of storage at 4 °C, as indicated by no statistically significant loss in cell-mediated or antibody responses (Figure 2a–c).

Mechanistically, simultaneous co-delivery of Poly(I:C) with adenovector vaccines impacted the proinflammatory microenvironment at the immunization site (Figure 2d–g). In particular, statistical analyses showed that the addition of Poly(I:C) significantly increased *IFNB1* (Figure 2d) and *CXCL10* (Figure 2e) expression at 6 hours with respect to blank (empty) MNAs or MNA-adenovirus vaccine alone, which suggests that Poly(I:C) plays a distinctive role during early skin immunomodulation. Furthermore, the inclusion of Poly(I:C) continued to significantly enhance the expression of *CXCL10* (Figure 2e) at later time points (24 hours and 48 hours) compared with the groups with blank MNA and MNA-adenovirus vaccine alone, consistent with a sustained chemoattractant effect of Poly(I:C). Importantly, these proinflammatory effects of Poly(I:C) correlate with enhanced systemic cytotoxic T-cell responses. Expression of the proinflammatory cytokines *IL1B* and *IL6*, which can be induced by a broad range of pathogen-associated molecular patterns and danger-associated molecular patterns, was elevated in MNA-immunized skin microenvironments at early time points (6 hours) regardless of vaccine components (Figure 2f and g) likely as a result of the mechanical stress of microneedle application. Interestingly, at later time points (48 hours and 72 hours), after the resolution of the transient mechanical stress generated by microneedles, both

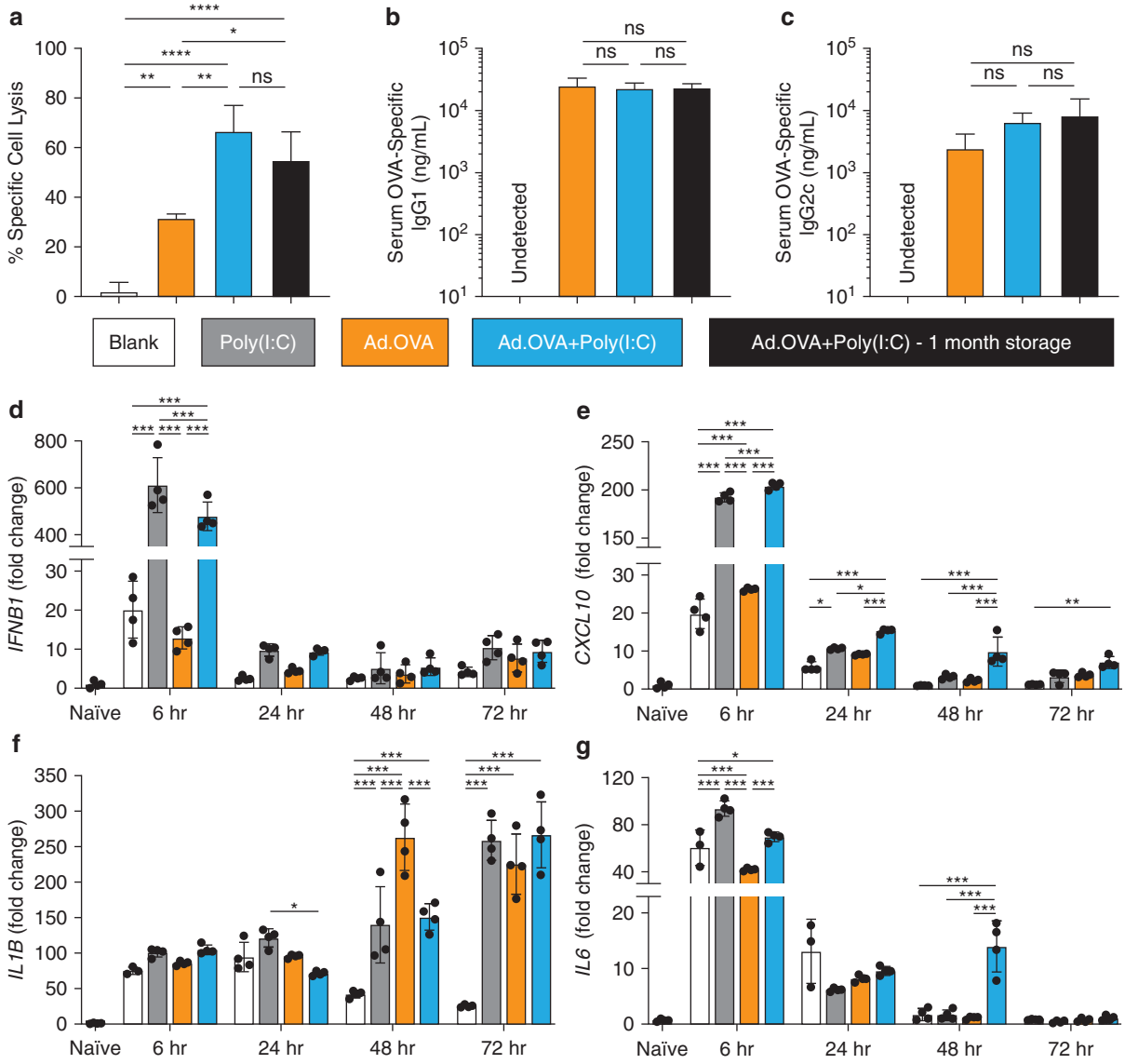

Figure 2. Intercutaneous immunization with multicomponent MNA vaccine platforms incorporating adenovector-encoded OVA and Poly(I:C) adjuvants more effectively engineers a proinflammatory skin microenvironment in vivo, promoting robust immune responses compared with immunization with MNA adenovector vaccine alone. Mice were immunized with Ad.OVA ± Poly(I:C) MNAs or blank MNAs (control). Antigen-specific cell-mediated and humoral immune responses were determined at the indicated time points using established lytic and ELISA assays, respectively. To assess the stability of multicomponent MNAs, intercutaneous immunization experiments were repeated with Ad.OVA+Poly(I:C) MNAs stored at 4 °C for 1 month. **(a)** Quantification of OVA-specific lytic responses. **(b, c)** Quantification of serum concentrations of OVA-specific IgG1 and IgG2c antibodies, respectively. Data are presented as mean ± SD and analyzed by one-way ANOVA, followed by Tukey's post-hoc test. ns > 0.05, $*P < 0.05$, $**P < 0.01$, $****P < 0.0001$. **(d–g)** To investigate key immune mediators in the skin microenvironment induced by immunization, MNAs with the indicated components or blank MNAs were applied as described above, and expression of **(d)** *IFNB1*, **(e)** *CXCL10*, **(f)** *IL1B*, and **(g)** *IL6* mRNA levels was quantified by RT-qPCR at the indicated time points. Data are presented as mean ± SD and analyzed by two-way ANOVA, followed by Tukey's multiple comparisons test. Significant differences between treatment groups at each time point are indicated by $*P < 0.05$, $**P < 0.01$, $***P < 0.001$. MNA, microneedle array; ns, nonsignificant; OVA, ovalbumin.

adenovirus and/or Poly(I:C) evoked significant increases in *IL1B* expression in the skin microenvironment, and the combination of Ad.OVA and Poly(I:C) sustained elevated levels of *IL6* through 48 hours.

Collectively, our results demonstrate improved immunogenicity of skin-targeted adenovector vaccines by simultaneous co-delivery of the TLR3 ligand Poly(I:C) and support further development of pathogen-associated molecular pattern and/or danger-associated molecular pattern ligand integration in MNA-delivered viral vector vaccines. Specifically, our results demonstrate that Poly(I:C)-adjuvanted MNA-adenovirus vaccines elicit significantly improved cytotoxic T-cell responses compared with adenovirus alone while generating antibody responses at least as good as adenovirus alone. MNA-delivered vaccines have the potential to offer advantages of ease of fabrication, application, and storage compared with other vaccine delivery platforms. Our results suggest that by uniquely enabling delivery of both adjuvant and antigen-encoding viral vectors to the same skin microenvironment, multicomponent MNA vaccine platforms result in improved immunogenicity, including cellular immune responses, thereby contributing to the

efforts to develop universal vaccines and improve global immunization capabilities.

Data availability statement

Data related to this article are available on request.

ORCIDs

Geza Erdos: http://orcid.org/0000-0001-7530-7371
Stephen C. Balmert: http://orcid.org/0000-0002-4938-0329
Cara Donahue Carey: http://orcid.org/0000-0002-3602-099X
Gabriel D. Falo: http://orcid.org/0000-0002-1669-8701
Nikita A. Patel: http://orcid.org/0000-0002-7162-9135
Jiying Zhang: http://orcid.org/0000-0002-4344-9794
Andrea Gambotto: http://orcid.org/0000-0001-8154-7419
Emrullah Korkmaz: http://orcid.org/0000-0002-8808-5445
Louis D. Falo Jr: http://orcid.org/0000-0001-9813-0433

CONFLICT OF INTEREST

GE and LDF are inventors of related intellectual property.

ACKNOWLEDGMENTS

The authors acknowledge the Preclinical In Vivo Imaging Facility at the UPMC Hillman Cancer Center. SCB is supported by the National Institutes of Health training grant T32-CA175294. AG is supported by the National Institutes of Health grant R21-AI130180, and LDF is supported by the National Institutes of Health grants R01-AR074285, R01-AR071277, and R01-AR068249.

AUTHOR CONTRIBUTIONS

Conceptualization: GE, LDF; Data Curation: GE, SCB; Formal Analysis: GE, SCB, GDF; Funding Acquisition: AG, LDF; Investigation: GE, SCB, CDC, GDF, NAP, JZ; Methodology: GE, EK, LDF; Project Administration: LDF; Resources: AG, LDF; Visualization: GE, SCB, EK, LDF; Writing - Original Draft Preparation: GE, SCB, EK; Writing-review and editing: GE, SCB, CDC, GDF, NAP, JZ, AG, EK, LDF

Geza Erdos[1], Stephen C. Balmert[1], Cara Donahue Carey[1], Gabriel D. Falo[1], Nikita A. Patel[1], Jiying Zhang[1], Andrea Gambotto[2,3,4], Emrullah Korkmaz[1,5] and Louis D. Falo Jr.[1,5,6,7,8,]*

[1]*Department of Dermatology, University of Pittsburgh School of Medicine, Pittsburgh, Pennsylvania, USA;* [2]*Department of Surgery, University of Pittsburgh School of Medicine, Pittsburgh, Pennsylvania, USA;* [3]*Department of Molecular Genetics and Biochemistry, University of Pittsburgh School of Medicine, Pittsburgh, Pennsylvania, USA;* [4]*Department of Medicine, University of Pittsburgh School of Medicine, Pittsburgh, Pennsylvania, USA;* [5]*Department of Bioengineering, University of Pittsburgh Swanson School of Engineering, Pittsburgh, Pennsylvania, USA;* [6]*Clinical and Translational Science Institute, University of Pittsburgh, Pittsburgh, Pennsylvania, USA;* [7]*The UPMC Hillman Cancer Center, Pittsburgh, Pennsylvania, USA; and* [8]*The McGowan Institute for Regenerative Medicine, University of Pittsburgh, Pittsburgh, Pennsylvania, USA*

[*]*Corresponding author e-mail: lof2@pitt.edu*

SUPPLEMENTARY MATERIAL

Supplementary material is linked to the online version of the paper at www.jidonline.org, and at https://doi.org/10.1016/j.jid.2020.03.966.

REFERENCES

Bachy V, Hervouet C, Becker PD, Chorro L, Carlin LM, Herath S, et al. Langerin negative dendritic cells promote potent CD8+ T-cell priming by skin delivery of live adenovirus vaccine microneedle arrays. Proc Natl Acad Sci USA 2013;110:3041–6.

Boehme KW, Compton T. Innate sensing of viruses by toll-like receptors. J Virol 2004;78:7867–73.

Condon C, Watkins SC, Celluzzi CM, Thompson K, Falo LD Jr. DNA-based immunization by in vivo transfection of dendritic cells. Nat Med 1996;2:1122–8.

DeMuth PC, Li AV, Abbink P, Liu J, Li H, Stanley KA, et al. Vaccine delivery with microneedle skin patches in nonhuman primates. Nat Biotechnol 2013;31:1082–5.

He Y, Zhang J, Donahue C, Falo LD Jr. Skin-derived dendritic cells induce potent CD8(+) T cell immunity in recombinant lentivector-mediated genetic immunization. Immunity 2006;24:643–56.

Herold S, Sander LE. Toward a universal flu vaccine. Science 2020;367:852–3.

Kabashima K, Honda T, Ginhoux F, Egawa G. The immunological anatomy of the skin. Nat Rev Immunol 2019;19:19–30.

Kashem SW, Haniffa M, Kaplan DH. Antigen-presenting cells in the skin. Annu Rev Immunol 2017;35:469–99.

Kim E, Erdos G, Huang S, Kenniston T, Falo LD Jr, Gambotto A. Preventative vaccines for zika virus outbreak: preliminary evaluation. EBioMedicine 2016;13:315–20.

Kim YC, Park JH, Prausnitz MR. Microneedles for drug and vaccine delivery. Adv Drug Deliv Rev 2012;64:1547–68.

Korkmaz E, Friedrich EE, Ramadan MH, Erdos G, Mathers AR, Ozdoganlar OB, et al. Therapeutic intradermal delivery of tumor necrosis factor-alpha antibodies using tip-loaded dissolvable microneedle arrays. Acta Biomater 2015;24:96–105.

Schijns VEJC, O'Hagan D. *Immunopotentiators in Modern Vaccines*. Amsterdam, Netherlands: Elsevier; 2006.

Sullivan SP, Koutsonanos DG, Del Pilar Martin MP, Lee JW, Zarnitsyn V, Choi SO, et al. Dissolving polymer microneedle patches for influenza vaccination. Nat Med 2010;16:915–20.

Vrdoljak A, McGrath MG, Carey JB, Draper SJ, Hill AVS, O'Mahony C, et al. Coated microneedle arrays for transcutaneous delivery of live virus vaccines. J Control Release 2012;159:34–42.

Zaric M, Becker PD, Hervouet C, Kalcheva P, Doszpoly A, Blattman N, et al. Skin immunisation activates an innate lymphoid cell-monocyte axis regulating CD8$^+$ effector recruitment to mucosal tissues. Nat Commun 2019;10:2214.

A Nitric Oxide–Releasing Topical Medication as a Potential Treatment Option for Atopic Dermatitis through Antimicrobial and Anti-Inflammatory Activity

Journal of Investigative Dermatology (2020) **140,** 2531–2535; doi:10.1016/j.jid.2020.04.013

TO THE EDITOR

Atopic dermatitis (AD) is a common, chronic inflammatory skin condition characterized by intense pruritis and recurrent eczematous lesions (Weidinger and Novak, 2016). An unmet medical need exists for a

Abbreviations: AD, atopic dermatitis; Th, T helper type

Accepted manuscript published online 16 May 2020; corrected proof published online 5 July 2020

SUPPLEMENTARY MATERIALS AND METHODS

Fabrication of microneedle arrays

Dissolving microneedle arrays (MNAs) with obelisk-shaped needles that incorporate adenovectors with or without Poly(I:C) were manufactured using our previously described MNA fabrication strategy (Korkmaz et al., 2015). Our MNAs are designed for human applications and are currently being used in phase I clinical trial for the treatment of cutaneous T-cell lymphoma (ClinicalTrials.gov #NCT02192021). Our fabrication methods are flexible to rapidly modify the microneedle and array designs for application-driven optimization (Balmert et al., 2020; Bediz et al., 2014). Briefly, MNA production molds were prepared using polydimethylsiloxane (SYLGARD 184 from Dow Corning, Midland, MI; 10:1 base material to curing agent ratio) through elastomer micromolding with MNA master molds that include 750 μm high microneedles in a 10 × 10 array configuration. We previously demonstrated that the same MNAs can deliver cargos to antigen-presenting cell-rich skin microenvironments in both mice and humans (Bediz et al., 2014). Next, polydimethylsiloxane production molds were used to fabricate dissolvable MNAs integrating Ad5.OVA (2×10^9 genome count per MNA) ± Poly(I:C) (100 μg per MNA) through a multi-step spin-casting technique. Sequential loading of Poly(I:C) and Ad5.OVA was performed through centrifugation at 4 °C and 3500 r.p.m. for 1 hour for each loading. After loading biocargos, the structural material of MNAs, prepared by dissolving carboxymethyl cellulose (cat# C5678, Sigma-Aldrich, St Louis, MO) and trehalose (cat# T9531, Sigma-Aldrich) powders in endotoxin-free water (HyClone Cell Culture Grade Water) at 15% w/w and 10% w/w, respectively, resulting in 25% w/w final solute concentration, was loaded onto polydimethylsiloxane production molds (75 μl of carboxymethyl cellulose/Treh hydrogel per MNA) and centrifuged at 10 °C and 3500 r.p.m. for 6 hours. Furthermore, blank MNAs without any biocargo were prepared from the same material composition for control experiments. Fabricated MNAs were imaged with a bright-field stereo microscope.

Fluorescent labeling

Adenovirus and Poly(I:C) were labeled using Alexa Fluor 555 and 488 fluorescent dyes, respectively. To label viral capsids, amine-reactive Alexa 555 dye (cat# A20009, ThermoFisher, Waltham, MA) was used according to the manufacturer's instructions with a minor modification, which is the direct solubilization of Alexa 555 dye in the viral suspension, avoiding the use of dimethylformamide that may impart detrimental effects on the capsid structure. To label Poly(I:C), its amine modification was performed as previously described (Hermanson et al., 1996). Briefly, 5 mg/ml Poly(I:C) was denatured at 95 °C for 5 minutes and reacted to 3 M ethylenediamine in the presence of 1 M sodium bisulfite at 42 °C for 3 hours. The reaction mix was dialyzed overnight at 4 °C. The resultant aminated Poly(I:C) was ethanol precipitated, air dried, and resuspended in water. Finally, amine-reactive Alexa-488 N-hydroxysuccinimide ester (cat#: A2000, ThermoFisher) was used to label NH_2-Poly(I:C) conjugate according to the manufacturer's instructions.

Mice and animal husbandry

C57BL/6J mice were purchased from The Jackson Laboratory (Bar Harbor, ME), maintained under specific pathogen-free conditions at the University of Pittsburgh, Pittsburgh, Pennsylvania, and used at 8–10 weeks of age in accordance with Institutional Animal Care and Use Committee-approved protocols and guidelines.

In vivo imaging

MNA-mediated skin-targeted co-delivery of Ad5.OVA and Poly(I:C) was demonstrated on a C57BL/6J mouse. MNAs integrating Alexa555-Ad5.OVA and Alexa488-Poly(I:C) were created as described above, applied to the ear of an anesthetized mouse for 10 minutes, and then removed. The mouse was imaged with an in vivo live animal imaging system (IVIS 200, PerkinElmer, Waltham, MA) to detect Alexa488-Poly(I:C) and Alexa555-Ad5.OVA at the MNA application site. Then, images were postprocessed using Living Image software (PerkinElmer).

Quantification of cytotoxic T-cell and antibody responses

Antigen (OVA)-specific cell-mediated immunity was determined by evaluating OVA-specific cell lysis in groups of four female C57BL/6J mice that were immunized by ear applications of Ad.OVA-MNAs, Ad.OVA+Poly(I:C)-MNAs, or blank MNA (control). Twelve days after immunization, mice were assayed for OVA-specific T-cell lytic activity using well-established techniques (Morelli et al., 2005). Briefly, splenocytes from naive mice were pulsed with 2 μg/ml OVA-derived SIINFEKL peptide epitope or left unpulsed for 1 hour. The unpulsed splenocytes were labeled with low-concentration Crystal Field Stabilization Energy (CFSE) (1 μM) for 15 minutes at 37 °C, whereas the antigen-pulsed splenocytes were washed and stained with high-concentration CFSE (10 μM). Equal populations of the pulsed and unpulsed target cells (2×10^7 splenocytes per mouse) were injected intravenously into immunized and naive mice. Twenty hours after the injection, the spleens were recovered from all the animals and the killing of target cells was evaluated by comparison of the antigen-pulsed and -unpulsed populations by flow cytometry to quantify antigen-specific killing of the high CFSE-labeled SIINFEKL-pulsed targets. Specific lysis was calculated according to the following formula: {1 − [(ratio of CFSElow/CFSEhigh of naive mouse)/(ratio of CFSElow/CFSEhigh of vaccinated mouse)]} × 100 and expressed as percentage of maximum lysis.

Antigen (OVA)-specific antibody responses were determined in groups of four female C57BL/6J mice that were immunized by ear applications of Ad.OVA-MNAs, Ad.OVA+Poly(I:C)-MNAs, or blank MNA (control). Thirty days after immunization, the standard curves for OVA-specific IgG1 and IgG2 antibodies were obtained, blood was collected cardiac puncture from anesthetized mice at the time of sacrifice by, serum was isolated using BD Microtainer serum separator tubes (BD Biosciences, San Jose, CA) and diluted to the levels within the standard curves to quantify OVA-specific IgG1 and IgG2c antibodies in serum by indirect ELISAs as previously described (Balmert et al., 2020).

Intercutaneous immunization experiments were repeated with Ad.OVA+Poly(I:C) loaded MNAs stored at 4 °C for 1 month, and the associated quantification of cell-mediated and humoral-immune responses was again performed as described above.

Real-time RT-qPCR

MNA-treated ear tissue was recovered after 6, 24, 48, and 72 hours and analyzed for specific gene expression of immune mediators by RT-qPCR. Skin was homogenized at 4 °C in TRI-reagent (Molecular Research Center, Cincinnati, OH) using a Bullet Blender Storm 24 with stainless steel beads in Navy RINO tubes (Next Advance, Averill Park, NY). Total RNA was extracted according to the manufacturer's protocol and quantified using a DeNovix DS-11 spectrophotometer (Wilmington, DE). For each reverse transcription reaction, 2 μg RNA was converted to cDNA using a QuantiTect Reverse Transcription Kit (Qiagen, Germantown, MD). Then, RT-qPCR was performed using TaqMan Fast Advanced Master Mix (Thermo Fisher) according to manufacturer's instructions with TaqMan Gene Expression assays (Applied Biosystems, Carlsbad, CA) that are specific for *IFNB1* (Mm00439552_s1), *CXCL10* (Mm00445235_m1), *IL1B* (Mm00434228_m1), and *IL6* (Mm00446190_m1). Target gene primer-probe assays were FAM-MGB labeled, whereas the *ACTB* endogenous control primer-probe assay (Mm00607939_s1) was VIC-MGB_PL labeled. Duplex reactions (target gene plus *ACTB*) were analyzed on a StepOnePlus Real-Time PCR System (Applied Biosystems). Expression of each target gene was calculated and normalized to the *ACTB* endogenous control and naive ear skin on the basis of the Livak ($2^{-\Delta\Delta Ct}$) method. The relative quantities were expressed as fold differences relative to naive skin.

Statistical analysis

GraphPad Prism v8 (San Diego, CA) software was used for statistical analyses. Data were represented as mean ± SD and analyzed by either one-way ANOVA followed by Tukey's post-hoc tests (Figure 2a–c) or two-way ANOVA followed by either Sidak's (Figure 1f) or Tukey's (Figure 2d–g) multiple comparison test. $*P < 0.05$, $**P < 0.01$, $***P < 0.001$, $****P < 0.0001$.

SUPPLEMENTARY REFERENCES

Balmert SC, Carey CD, Falo GD, Sethi SK, Erdos G, Korkmaz E, et al. Dissolving undercut microneedle arrays for multicomponent cutaneous vaccination. J Control Release 2020;317:336–46.

Bediz B, Korkmaz E, Khilwani R, Donahue C, Erdos G, Falo LD, et al. Dissolvable microneedle arrays for intradermal delivery of biologics: fabrication and application. Pharm Res 2014;31:117–35.

Hermanson GT. Nucleic acid and oligonucleotide modification and conjugation. In: Bioconjugate techniques. Cambridge, MA: Academic Press; 1996. p. 639–71.

Korkmaz E, Friedrich EE, Ramadan MH, Erdos G, Mathers AR, Ozdoganlar OB, et al. Therapeutic intradermal delivery of tumor necrosis factor-alpha antibodies using tip-loaded dissolvable microneedle arrays. Acta Biomater 2015;24:96–105.

Morelli AE, Rubin JP, Erdos G, Tkacheva OA, Mathers AR, Zahorchak AF, et al. CD4+ T cell responses elicited by different subsets of human skin migratory dendritic cells. J Immunol 2005;175:7905–15.